

**UCC Library and UCC researchers have made this item openly available.  
 Please [let us know](#) how this has helped you. Thanks!**

<b>Title</b>	Electroless thin film CoNiFe-B alloys for integrated magnetics on Si
<b>Author(s)</b>	Rohan, James F.; Ahern, Bernadette M.; Reynolds, Ken; Crowley, Stephan; Healy, David A.; Rhen, Fernando M. F.; Roy, Saibal
<b>Publication date</b>	2009-02-15
<b>Original citation</b>	ROHAN, J. F., AHERN, B. M., REYNOLDS, K., CROWLEY, S., HEALY, D. A., RHEN, F. M. F. & ROY, S. 2009. Electroless thin film CoNiFe-B alloys for integrated magnetics on Si. <i>Electrochimica Acta</i> , 54 (6), 1851-1856. <a href="http://dx.doi.org/10.1016/j.electacta.2008.10.019">http://dx.doi.org/10.1016/j.electacta.2008.10.019</a>
<b>Type of publication</b>	Article (peer-reviewed)
<b>Link to publisher's version</b>	<a href="http://www.sciencedirect.com/science/article/pii/S001346860801222X">http://www.sciencedirect.com/science/article/pii/S001346860801222X</a> <a href="http://dx.doi.org/10.1016/j.electacta.2008.10.019">http://dx.doi.org/10.1016/j.electacta.2008.10.019</a> Access to the full text of the published version may require a subscription.
<b>Rights</b>	<b>Copyright © 2009 Elsevier Inc. All rights reserved. NOTICE: this is the author's version of a work that was accepted for publication in <i>Electrochimica Acta</i>. Changes resulting from the publishing process, such as peer review, editing, corrections, structural formatting, and other quality control mechanisms may not be reflected in this document. Changes may have been made to this work since it was submitted for publication. A definitive version was subsequently published in <i>Electrochimica Acta</i> [Volume 54, Issue 6, 15 February 2009, Pages 1851–1856]  <a href="http://dx.doi.org/10.1016/j.electacta.2008.10.019">http://dx.doi.org/10.1016/j.electacta.2008.10.019</a></b>
<b>Item downloaded from</b>	<a href="http://hdl.handle.net/10468/1652">http://hdl.handle.net/10468/1652</a>

Downloaded on 2021-11-30T23:30:34Z

## Electroless thin film CoNiFe-B alloys for integrated magnetics on Si.

James F. Rohan<sup>a,\*</sup>, Bernadette M. Ahern<sup>a</sup>, Ken Reynolds<sup>a</sup>, Stephan Crowley<sup>b</sup>, David A. Healy<sup>b</sup>, Fernando M. F. Rhen<sup>a</sup> and Saibal Roy<sup>a</sup>.

<sup>a</sup> Tyndall National Institute, University College Cork, Lee Maltings, Prospect Row, Cork, Ireland.

<sup>b</sup> Chemistry Department, University College Cork, Ireland

---

\* Corresponding author. Tel.: +353 21 4904224; fax: +353 21 4270271.

*E-mail address:* [james.rohan@tyndall.ie](mailto:james.rohan@tyndall.ie) (James F. Rohan)

<sup>1</sup> ISE member

## **Abstract.**

Electroless magnetic thin films have been deposited from borane based baths suitable for use in integrated magnetics on Si applications. The baths were developed for compatibility with standard photoresist for microfabrication of integrated magnetics on Si. The specific formulations, which differ from those reported previously, yield uniform, high saturation magnetisation (up to 2.15 T) deposits with low coercivity (< 2 Oe). The resistivity of the film can be increased to minimise eddy current losses by using higher dimethylamine borane (DMAB) content or the inclusion of a second reducing agent, hypophosphite, to facilitate phosphorus codeposition of up to 7 at. %. The Ni content in the plating bath has been shown to exert significant influence over the composition, deposition rate and coercivity. XRD analysis suggests that the deposits consist of nanocrystalline phase with grains < 20 nm. Such small grains are consistent with the observed low coercivity of the deposits.

Key words.

Electroless, magnetic, borane, coercivity, resistivity.

.

## 1. Introduction

Electrochemical deposition of metals and alloys is well suited to microfabrication on Si that requires high speed and selective deposition on patterned substrates. This has been demonstrated by the development of microfabricated devices with magnetic core materials such as integrated motors [1], microactuators [2], relays [3], microinductors [4] and microtransformers.[5.6] NiFe [7, 8] materials exhibit many of the desirable characteristics for integrated micromagnetic devices such as microinductors, i.e. low coercivity ( $<2$  Oe) for operation at the target 1-10 MHz frequencies, high saturation flux density ( $B_{\text{sat}}$ ), (e.g. up to 1.6 T for  $\text{Ni}_{45}\text{Fe}_{55}$ ) to facilitate the use of thin films and resistivities greater than  $20 \mu\Omega \text{ cm}$  to reduce eddy current losses in the magnetic material and improve the overall efficiency of the device. More recently Co containing alloys (CoNiFe [9-12] and CoFe [13, 14]) have been investigated as these materials exhibit larger saturation magnetisation values approaching the maximum achievable for bulk materials, 2.43 T. [15-17]

To further facilitate microfabrication and integration on Si the development of suitable electrolessly deposited magnetic materials has been investigated in this work. Electroless deposition has the advantages over electrodeposition of potentially yielding selective, conformal deposits on three dimensional substrate topology without the need for blanket conductive seed layers. This can simplify the processing route in any given microfabrication approach. For example, it can be utilised on prepatterned seed layers eliminating the need to expose the deposited magnetic materials to aggressive etch solutions which is the case when blanket seed layers are utilised. The etchants for adhesion and seed metal layers may also alter the surface

characteristics of the magnetic alloy deposit, which in turn may increase the coercivity [18]. The need for sophisticated cell design including optimised anode positioning to achieve uniform deposition thickness and composition is also eliminated.

The choice of plating bath composition depends on the application and in the present work high saturation magnetisation ( $B_{\text{sat}}$ ) is desirable together with low coercivity. A number of groups have recently reported the electroless deposition of magnetic materials. Osaka [19-21] and coworkers have investigated electroless magnetic alloys and shown that higher  $B_{\text{sat}}$  values can be obtained from deposits using dimethylamine borane (DMAB) rather than hypophosphite as the reducing agent. This has been attributed to differences in the crystallite structure and codeposited elements. They also found coercivity ( $H_c$ ) to be less than 2 Oe for deposits containing 13 at.% or less Ni with  $B_{\text{sat}}$  values of approximately 1.7 T. The microstructure of the deposit was determined to be fcc with grain sizes of 10-12 nm. CoNiP [22,23] has also been investigated but typically exhibits a relatively large coercivity (~60 Oe) which is beyond the application range in the current work. The  $B_{\text{sat}}$  value of 1.7 T is also the maximum achievable for this non-Fe containing alloy.

For these reasons we have focussed on DMAB based solutions with the goal of achieving higher  $B_{\text{sat}}$  values in combination with low coercivity. It was also a target of the present investigation to increase the resistivity of the deposits beyond that reported to date for electroless magnetic films from DMAB based baths while maintaining a high magnetisation and low coercivity. The purpose of this work was to determine the plating bath composition to achieve selective uniform composition and

thickness for electroless CoNiFe materials deposition from DMAB based baths for micromagnetics on Si applications which have been described previously for electrolytic magnetic materials deposition [4,6]. More specifically, alloys with the following improved combination of characteristics over those reported in the literature to date were targeted;

- coercivity  $< 2$  Oe,
- saturation magnetization larger than 2.0 T
- resistivity greater than  $25 \mu\Omega$  cm

and compatibility with standard photoresist patterning materials and mobile ion free solutions for microfabrication on Si applications.

## **2. Experimental**

All chemicals used were purchased from Sigma Aldrich and used as received. Deionised water of resistivity  $18 \text{ M}\Omega$  cm was used to prepare the solutions. The electroless solutions were prepared in glass beakers and the temperature maintained using an Ikamag RCT stirring hotplate with an Ikatron ETS-D4 electronic thermometer and IKA H 60 temperature probe. All experiments were performed with magnetic stirring at 100 rpm. The pH was adjusted using ammonium hydroxide. Teflon substrate holders were used. Si wafers with sputter coated patterned Ti adhesion layer (20 nm) and Cu seed layers (200 nm) were used as substrates. These metals were DC magnetron sputter coated using Nordiko equipment. A commercial positive photoresist, S1813, (approximately  $1.3 \mu\text{m}$  thick) supplied by Shipley was

used to pattern the substrates. The patterning was achieved on a Karl Suss MA 45 UV mask aligner.

The deposited material selectivity and morphology was analysed using a Hitachi S-400 field effect scanning electron microscope (SEM) with a PGT IMIX Energy Dispersive X-ray (EDX) system with intensity correction for elemental analysis of deposit composition given in atomic % (at.%) and uniformity. The EDX compositions were confirmed and the B content was determined by Inductively Coupled Plasma Atomic Emission Spectrometry (ICP AES) (Perkin Elmer, USA, Optical Emission Spectrometer Optima 2000 DV) to lie in the range 0.6 to 1.3 at. % for films deposited from electroless baths containing DMAB in the range 0.07 to 0.14 mol dm<sup>-3</sup>, respectively. The ICP-AES method of B analysis involved digesting the samples in a solution of 2 mls. ultrapure HNO<sub>3</sub>, 2 mls. millipure deionised water and 100 µl Ultrapure HF and testing against a SPEX CertiPrep Ltd standardised calibration solution. Deposit thickness and uniformity was determined using a Tencor Alpha-Step 200 surface profilometer and correlated with data measurements recorded on the SEM. The bath compositions are listed in table 1.

Electrical resistivity values were measured with a four point probe connected to a GW Laboratory DC current source and two PREMA 5017 Digital Multimeters. Currents of 50-150 mA were applied to the sample within the voltage limit and the resistivity calculated as:  $\rho = K \left( \frac{V}{I} \right) t$ , where t is the alloy thickness and K the measured sheet resistance correction factor for the sample size (4.53 for a full wafer). X-ray diffraction analysis was performed on a PANalytical X'Pert PRO MPD equipped with

Cu K-alpha radiation ( $1.5405\text{\AA}$ ) source. Stoller slits of 0.2 degrees were used, with a goniometer resolution of 0.001 degrees. The ternary alloy was annealed at  $450^{\circ}\text{C}$  for 5 hours in a Carbolite TZF ( $1200^{\circ}\text{C}$  Horizontal Three Zone Tube) Furnace to examine the influence of the anneal on the XRD pattern achieved.

Room temperature static magnetic properties of electroless deposited films were characterized using a BH loop tracer produced by SHB instruments. Magnetic measurements were carried out samples  $1 \times 1 \text{ cm}^2$  in size. Saturation magnetization values were determined at an applied field of 50 Oe. During sample preparation no external magnetic field was applied to the samples, however magnetic measurements reveal a degree of in plane anisotropy with clear easy and hard axis preferential directions. It is likely that some anisotropy is induced by the solution flow direction during the electroless process associated with magnetic stirring. Anisotropy behaviour has also been found in electroplated CoNiFe in an absence of an external magnetic field during plating [18].

### **3. Results and discussion**

#### *3.1 Alloy composition and deposition rate*

A number of electrolessly deposited CoNiFe materials have been reported [9, 10, 20] and the atomic percentage (at. %) compositions are typically Co (55-77), Ni (12-18) Fe (9-23) although a recent work [24] has highlighted Fe rich deposits such as  $\text{Co}_{33}\text{Ni}_{16}\text{Fe}_{46}\text{B}_1$  which may be achieved by developing electroless baths that have optimised levels of each of the metal ion sources, at least two complexing additive



materials and a suitable DMAB concentration. The electroless alloy plating baths developed in this work utilise DMAB as a reducing agent. CoNiFe materials were deposited at 2 to 4  $\mu\text{m/hr}$  from photoresist compatible solutions to enable selective deposition without a palladium or alternative activation pretreatment step. Preliminary investigations led to a stable bath formulation which differs from those in the literature. The bath compositions are listed in table 1.

It has been illustrated many times in the literature that the deposit composition and characteristics depend significantly on the bath composition. The specific complexing additives utilised in the present study were diammonium citrate and lactic acid. Preliminary bath composition analysis was accomplished to achieve CoNiFe bath compositions at the desired pH of 9 for compatibility with organic photoresist materials. The DMAB content was maintained at or below 0.14 M as accelerated hydrolysis may be observed in more concentrated solutions [25] particularly at the lower  $[\text{OH}] : [\text{DMAB}]$  ratio employed in the pH range of useful plating baths

Further development of the plating solution composition was performed to assess the role of the metal ions and reducing agents on the deposit composition and characteristics thereof. Fig. 1 (a) shows that varying the DMAB content does not have a significant influence on the deposit composition with all baths giving a deposit in the range Co (50 - 55), Ni (20 - 24) and Fe (22 - 25) at. %. The deposition of uniform and consistent films from a variety of borane concentration baths is beneficial in a plating environment as the borane concentration may be varied deliberately or inadvertently decrease during bath operation without exerting a significant influence on the deposit composition. The compositional analysis of the deposits also illustrates

the ‘anomalous’ deposition [26] where the less noble metal deposits preferentially. In this case, the less noble Co content in the deposit is more than double that of Ni while the ion concentration ratio in solution is only 1.3.

To modify the composition of the deposit in a well ordered manner it was found that varying either the Co or Ni content in the bath gave a systematic change in the deposit composition. The influence of increasing Ni ion content in the bath is shown in Fig. 1 (b) where the Ni content of the deposit was found by EDX to lie in the range 19 to 28 at %. The resulting deposits exhibited low coercivity which is discussed below. One target of the present investigation is  $B_{\text{sat}}$  value in excess of 1.7 T to compete with the processing and performance of electrolytic or vacuum deposited magnetic materials. It has been reported [12] that a higher Fe to Co ratio in electroplated deposits leads to higher  $B_{\text{sat}}$  values. DMAB based baths can codeposit significant quantities of Fe and therefore yield deposits with a relatively high  $B_{\text{sat}}$  value. In our work the Fe salt concentration was held constant at  $0.013 \text{ mol dm}^{-3}$  as each of the deposits achieved with this concentration had  $B_{\text{sat}}$  values in excess of 1.7 T. Higher concentrations of Fe in solution resulted in lower bath stability and lower concentrations did not yield the Fe content in the deposit required to maximise the  $B_{\text{sat}}$  of the alloy films.

While the DMAB content does not have a systematic influence on deposit composition, it does lead to a gradual increase in the deposition rate from 3.8 to 4.12  $\mu\text{m/hr}$  on doubling the DMAB concentration from 0.07 to 0.14  $\text{mol dm}^{-3}$ . The metal ion content again has a much larger influence on the deposition rate for the concentration ranges chosen with Ni having approximately 20 % more of an impact than Co on the deposition rate per unit added. This is illustrated in Fig. 2 and consistent with the

literature [26] which showed a higher catalytic activity for DMAB oxidation at Ni-B rather than Co-B substrates. To summarise the influence of each of the constituents on the deposition rate it can be concluded that over the useful concentration ranges investigated in this work the plating rate can be varied between 3.1 and 4.2  $\mu\text{m/hr}$ . This deposition rate is acceptable for the deposition of magnetic films in microfabricated devices such as microinductors where a deposit thickness of 1 - 5  $\mu\text{m}$  (depending on the frequency of operation) is required. The photoresists utilised have shown no issues with plating bath compatibility over this timeframe.

### 3.2 *Magnetic characteristics*

Coercivity is a measure of the field strength required to bring the magnetization of a material to zero. For microinductor and other applications, such as read/write heads for memory devices, a low value of coercivity or 'soft' magnetic properties is desirable. In the present study we found that increasing the DMAB content of the plating bath led to an increase in the coercivity of the deposits as shown in Fig. 3 (a). It is therefore desirable to operate the bath at low DMAB concentration, where values of coercivity less than 2 Oe were achieved. The increase in coercivity with increasing DMAB content may result from the incorporation of increased B content from the borane of the reducing agent. The B content determined by ICP-AES was 0.6 at. % for the 0.07  $\text{mol dm}^{-3}$  DMAB and increased to 1.3 at.% for the 0.14  $\text{mol dm}^{-3}$  DMAB solution. There is also likely to be increasing concentrations of adsorbing dimethylamine species [27] during the oxidation process which can lead to a more stressed deposit and higher coercivity. Varying the Co content had very little influence on the coercivity where  $\sim 2$  Oe was measured for each of the Co

concentrations investigated in the range 0.16 to 0.22 mol dm<sup>-3</sup>. Coercivity was found to be at a minimum for the highest concentration of Ni in the solutions, Fig. 3 (b). Based on these measurements it appears that, unlike the results described previously for electroless magnetic films [9], low coercivity may be achieved with greater than 13 at. % Ni in the deposit and in fact for these bath formulations, larger concentrations of Ni led to lower coercivity values. A number of interrelated factors may contribute to the coercivity, such as grain size, crystal structure, stress and surface roughness. It is expected that the higher content Ni baths which deposit at higher rates have smaller grain size and hence lower coercivity. It has been shown for electrolytically [9, 28] deposited CoNiFe films that the smallest grains (10 nm) and lowest coercivity (1.2 Oe) was achieved for mixed phase bcc/fcc deposits. Slightly larger 15 nm grains were measured for fcc phase deposits which exhibited coercivities of 2 Oe and the largest 20 nm grains were bcc phase. In those studies it was shown that the bcc phase is more evident at high Fe content and fcc phase dominant at low Fe content. In the present work this corresponds to bcc phase for low Ni content deposits and fcc more likely at higher Ni content based on the results presented in Figure 1 (b).

A relatively large  $B_{\text{sat}}$  value was achieved for a deposit at the optimised metal ion content and low DMAB content (0.07 mol dm<sup>-3</sup>). The coercivity of this deposit was also in the desirable (< 2 Oe) range based on the bcc/fcc ratio discussed above. The  $B_{\text{sat}}$  value decreased from 2.15 T to approximately 1.7 T as shown in Fig. 4 (a and b), when the DMAB content of the bath was doubled from 0.07 to 0.14 mol dm<sup>-3</sup>, yielding deposits of  $\text{Co}_{55}\text{Ni}_{21.4}\text{Fe}_{23}\text{B}_{0.6}$  and  $\text{Co}_{52}\text{Ni}_{24}\text{Fe}_{22.7}\text{B}_{1.3}$ , respectively. This is likely a result of the decreased Co and higher B content in the deposit from the higher

DMAB concentration bath. Taken in combination these results show that it is possible to achieve low coercivity, high  $B_{\text{sat}}$  deposits from electroless plating solutions in which specific bath formulations are utilised to achieve small grain size and optimised metal ion and impurity elements such as the B content. The concentration ranges for the bath constituents used in this work are quite different to those in the literature and it would appear that the various interactions of these bath constituents for ternary alloy deposition can yield materials with properties that differ from those reported to date. It may also be possible through the use of alternative complexing agents or metal ion and reducing agent materials to achieve further advances in the field of electroless magnetic alloy deposition.

### 3.3 *Resistivity*

The resistivity of the deposits is a significant parameter as it determines the thickness of the films that may be utilised before significant losses occur due to eddy current generation in the magnetic material. Such losses may be significant during device operation, particularly at the frequencies of the target application which lie in the 1 to 10 MHz range. Typical resistivity values achieved to date for electrolessly deposited magnetics are 20 to 40  $\mu\Omega$  cm. Among the significant contributors to resistivity in electroless films are the codepositing elements. The deposits resulting from oxidation of DMAB usually contain a low concentration of B (~1 at. %). Deposits from hypophosphite based baths exhibit higher resistivities (based on the higher phosphorus codeposit content of up to 12 at.%) but lower saturation magnetization ( $B_{\text{sat}}$ ) values because they do not deposit Fe containing alloys. Literature values also indicate that

hypophosphite baths yield deposits with much larger coercivities which are outside the useful operation range for the target applications described here.

The baseline material deposited in this work had a resistivity of approximately  $30 \mu\Omega$  cm. Increasing the Ni or Co content of the bath and of the deposit led to a decrease in the resistivity of the materials deposited to  $23 - 25 \mu\Omega$  cm. An increase in the resistivity of the materials deposited was observed when the DMAB concentration was doubled from  $0.07$  to  $0.14 \text{ mol dm}^{-3}$ . The maximum resistivity achieved was  $45 \mu\Omega$  cm as shown in Fig. 5. This may be attributed to B codeposition which increased in line with the DMAB content in the bath. It is undesirable to increase the DMAB content of the bath to achieve higher resistivities due to the increased coercivity discussed earlier. For such films an alternative approach that can increase resistivity is required. To achieve this while maintaining the essential elements of the plating bath hypophosphite co-reducing agent was also incorporated in the bath which may be catalytically oxidised at the depositing alloy while the DMAB affords the Fe content necessary for high  $B_{\text{sat}}$  values. The hypophosphite was introduced to the bath as the Ni salt (synthesised in-house) thereby maintaining the bath sodium or potassium ion-free for compatibility with Si processing. The use of Ni hypophosphite salt as the metal source and reducing agent has been described earlier [29].

The bath formulations used in this work are listed in table 1 above. The data in table 2 shows that incorporation of 2 at. % P in the deposit has very little influence on the deposit composition but increases the resistivity and easy axis coercivity while leading to a slight decrease in the  $B_{\text{sat}}$  values. This progression continues with an increase in the hypophosphite concentration in the bath to  $0.02 \text{ mol dm}^{-3}$  from  $0.0034 \text{ mol dm}^{-3}$  resulting in the codeposition of 4.5 at. % P. The deposit composition is also modified

substantially with Ni hypophosphite addition to the bath. The Ni content of the deposit increases (which is beneficial in maintaining a low coercivity) and both the Co and Fe concentrations decrease significantly. The sample with 7 at. % phosphorus had a large resistivity value based on the combined use of the highest DMAB concentration investigated in this work ( $0.14 \text{ mol dm}^{-3}$ ) and  $0.05 \text{ mol dm}^{-3}$  hypophosphite addition. However, the sample suffers greatly in terms of coercivity which is increased to greater than 12 Oe and furthermore the  $B_{\text{sat}}$  drops to 1.3 T as listed in table 2.

These experiments do show, however, that it is possible to increase the resistivity of the films to levels similar to those achieved with the highest concentration of DMAB ( $45 \mu\Omega \text{ cm}$ ) by the incorporation of phosphorus up to 4.5 at. % from a second reducing agent without a significant increase in coercivity ( $< 2 \text{ Oe}$ ) or decrease in the magnetisation ( $> 1.8 \text{ T}$ ). The deposition rate for the bath with concentrated borane + hypophosphite 3 in table 1 was also higher ( $6.8 \mu\text{m/hr}$ ) than for those with borane alone. However, it also contained more than twice the concentration of Ni ion than the other baths and the DMAB was at the highest level of  $0.14 \text{ mol dm}^{-3}$ . The other solutions listed in table 1 with added Ni hypophosphite had a total Ni ion concentration of  $0.02 \text{ mol dm}^{-3}$  which is only slightly higher than the baseline DMAB bath with  $0.017 \text{ mol dm}^{-3}$  Ni ions and each of these had a deposition rate in the 3 to 4  $\mu\text{m/hr}$  range.

### 3.4 *Microstructure*

Osaka [9] has described the use of plating baths without the typical sulphur containing additives which yielded decreased grain size films and thereby low coercivity.

Tabakovic [12] and Saito [30] have also linked small grain size with decreased coercivity values. In both cases they have identified the fcc rich phase of the ternary alloy as the main contributor to small grain size and the low coercivity desirable for 'soft' magnetic applications while the bcc phase contributes to the high  $B_{\text{sat}}$  value. XRD analysis of the deposits in this work did not yield significant peaks over the two theta range 10 to 90°. A broad shoulder shown in Fig. 6 is observed (43.9 to 45°) after the Cu substrate peak at 43.37° for the magnetic material  $\text{Co}_{55}\text{Ni}_{21.4}\text{Fe}_{23}\text{B}_{0.6}$ . The shoulder grew in intensity upon annealing the sample at 450°C under a nitrogen atmosphere for 5 hours. The emergence of the diffraction peak at 44.2° following the extended anneal would seem to indicate that the fcc phase is predominant. Using the Debye-Scherrer formula, the calculated grain size remains smaller than 20 nm even following the anneal. Therefore, the deposit may be considered to be nanocrystalline. This is in line with the grain size determined by other researchers for electrolytically deposited CoNiFe alloys and is consistent with the low coercivity values recorded in this work.

#### **4. Conclusions**

The electroless magnetic films deposited in this work have achieved coercivity and saturation magnetisation values that are competitive with electrolytic magnetic materials deposition. This study has also shown the influence of the key parameters on the films deposited, i.e. borane, Co and Ni ion concentration. The films have been deposited from baths that are alkali metal ion free even upon the addition of hypophosphite to increase the resistivity and are thereby compatible with Si microfabrication. The resistivity of the film can be increased by using higher DMAB



content or the inclusion of a second reducing agent hypophosphite to facilitate P codeposition up to a level of 7 at %. The Ni content in the plating bath has been shown to exert significant influence over the deposit composition, rate and coercivity. It is suggested that the deposits are nanocrystalline with the small grain size (~20 nm) leading to the observed low coercivity for the deposits. The baths operate at relatively low temperature and at pH values compatible with standard photoresists used in the microfabrication of magnetic components such as microinductors on Si. The next phase of this work is to investigate the optimised formulation in microinductor devices to assist with the achievement of low cost integrated magnetic components on Si for power supply on chip applications.

### **Acknowledgements**

This work was part funded under the EU Framework V Growth program project no. G1RD-CT-2000-00427.

SR would like to acknowledge Science Foundation Ireland Principal Investigator (SFI-PI) Grant no. 06/IN.1/I98.

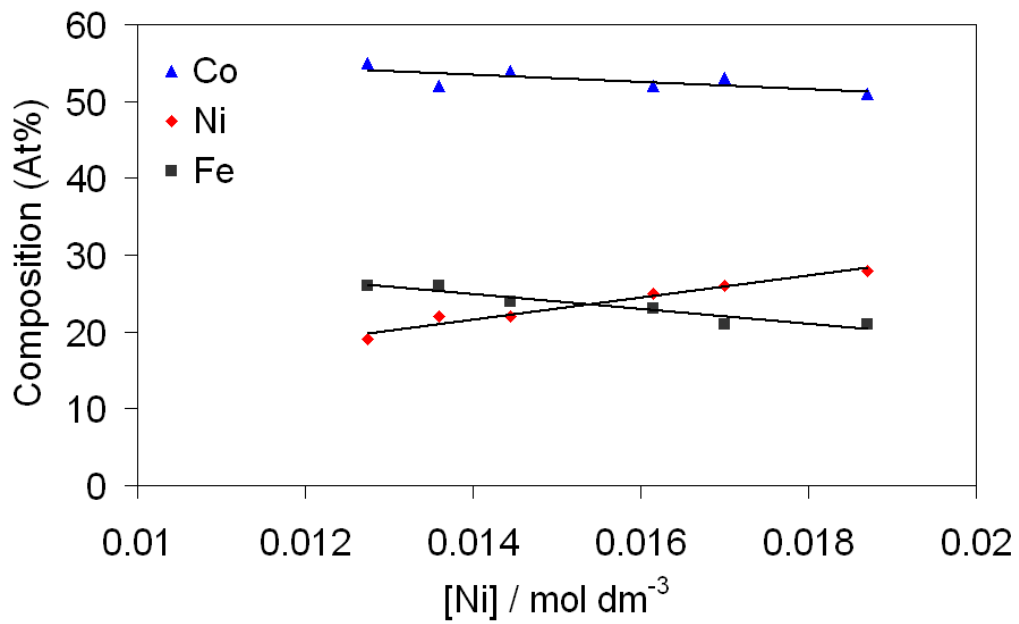
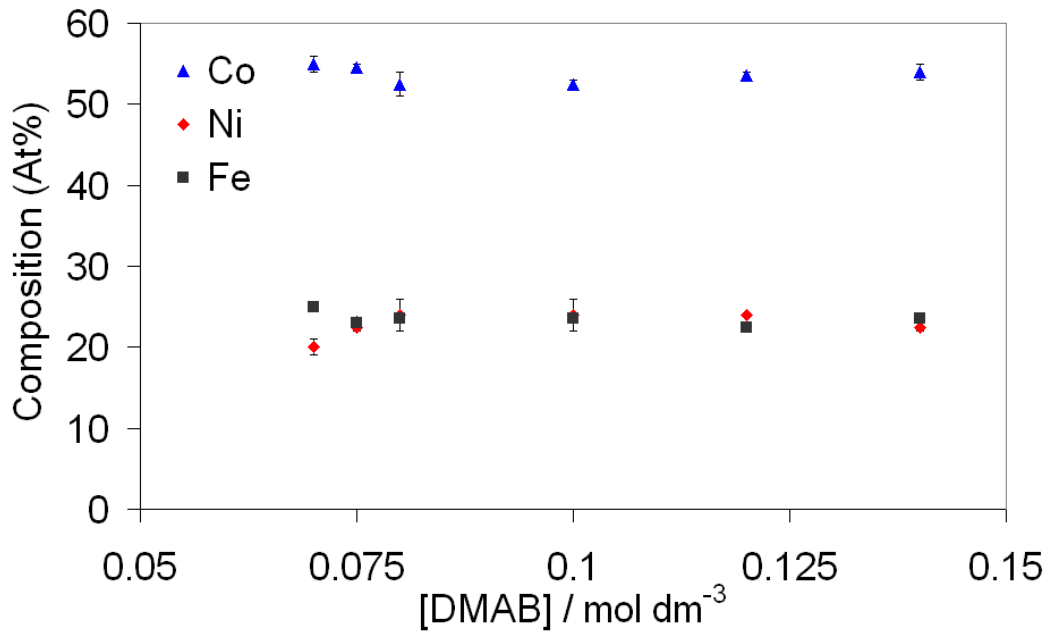


Figure 1. Deposit composition for the alloy as a function of the (a) DMAB content in the bath and (b) Ni ion concentration.

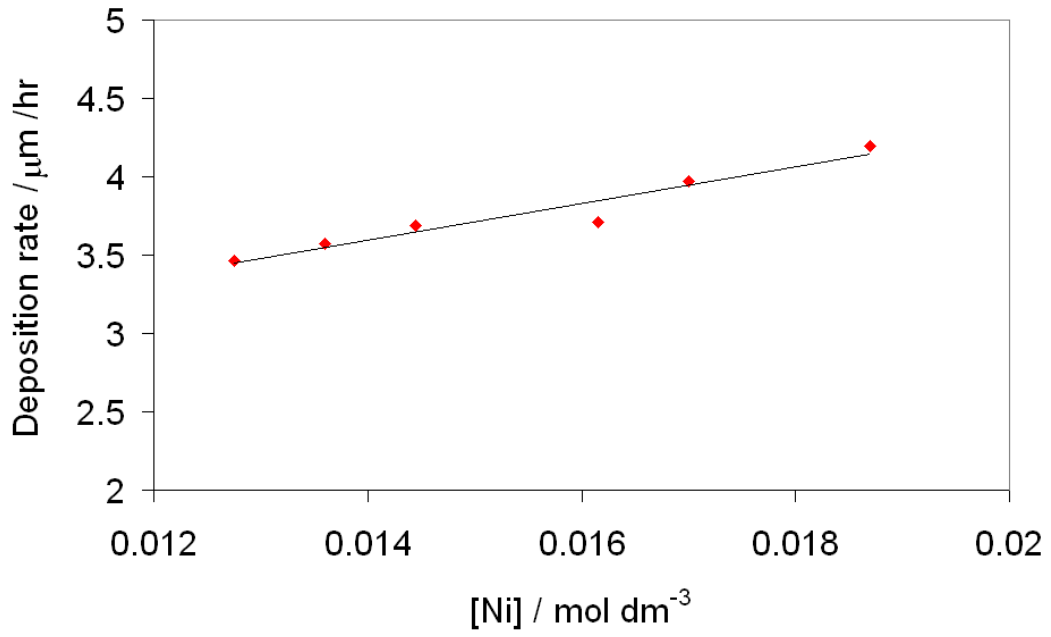
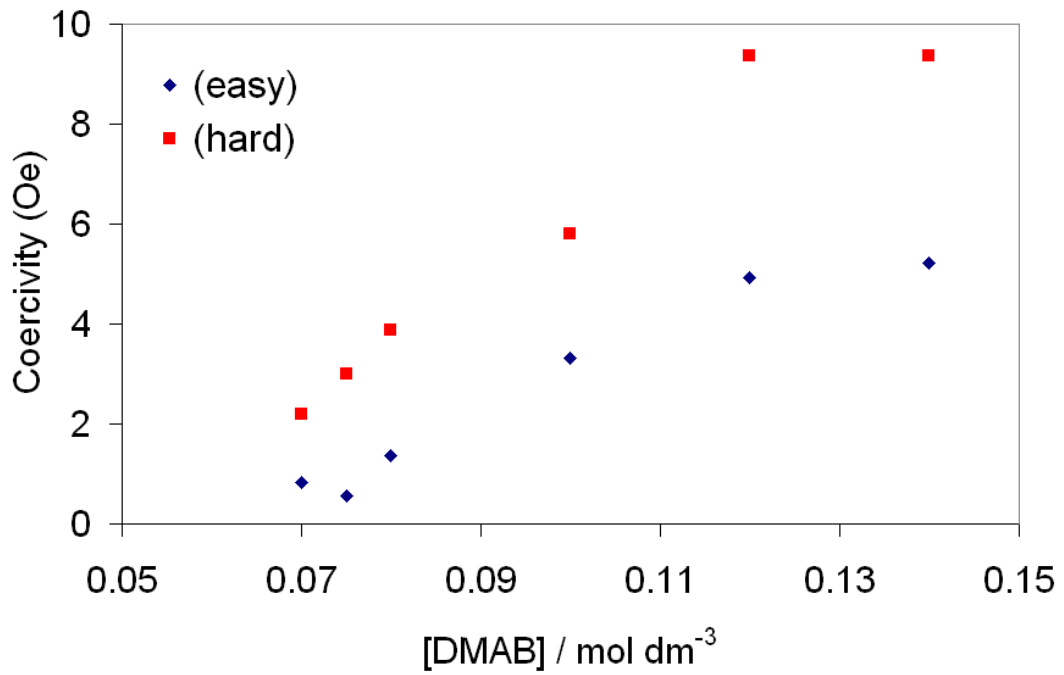


Figure 2. Influence of Ni ion content in the bath on the deposition rate for the deposited alloys.



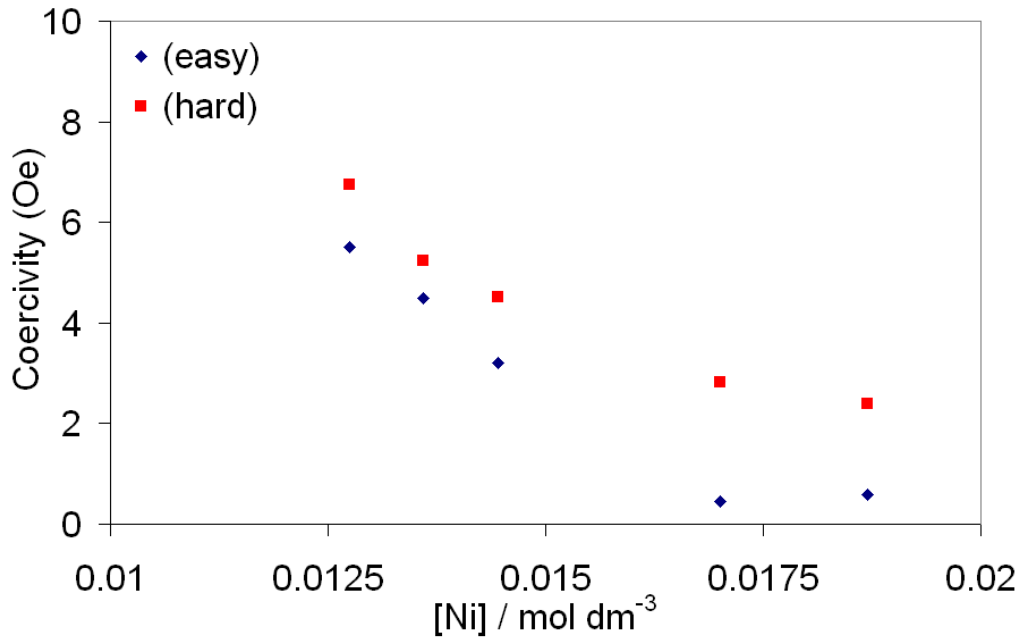


Figure 3 Influence of (a) DMAB concentration and (b) Ni ion concentration on the coercivity of the deposited alloy films.

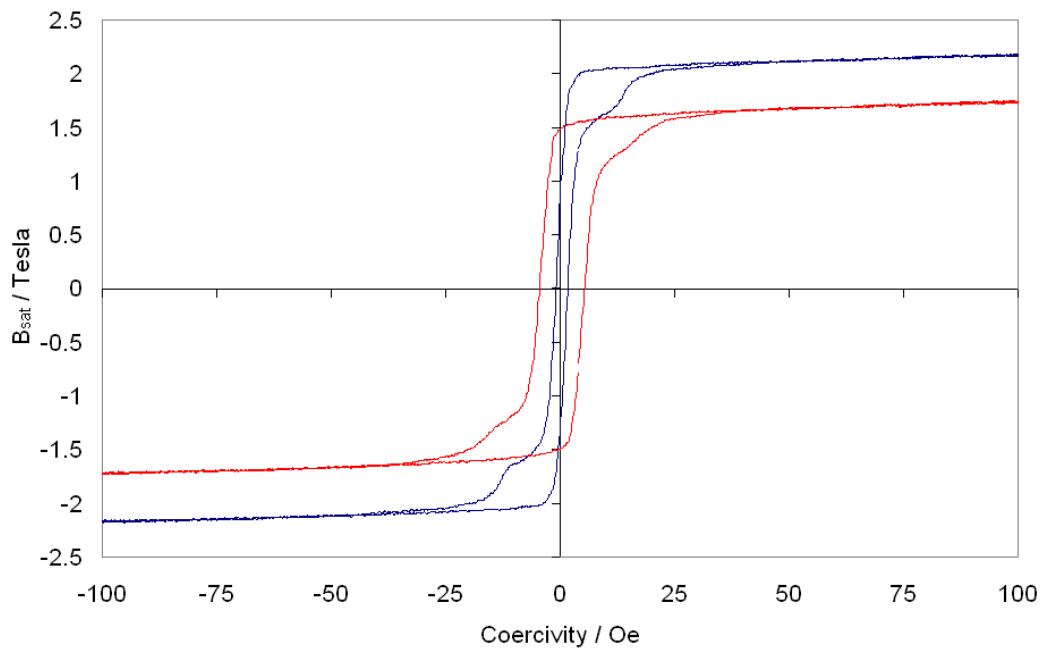


Figure 4. Magnetisation data for samples deposited (a) from 0.07 mol dm<sup>-3</sup> and (b) 0.14 mol dm<sup>-3</sup> DMAB solutions.

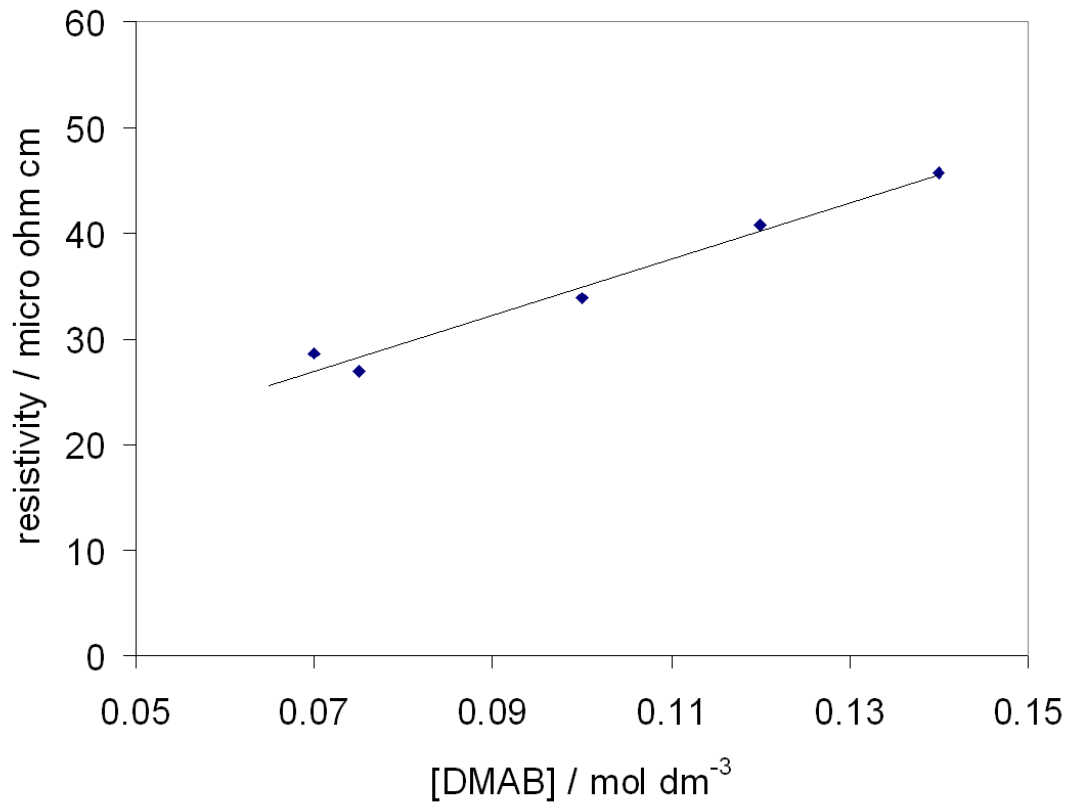


Figure 5. Increasing film resistivity as a result of increased DMAB bath content.

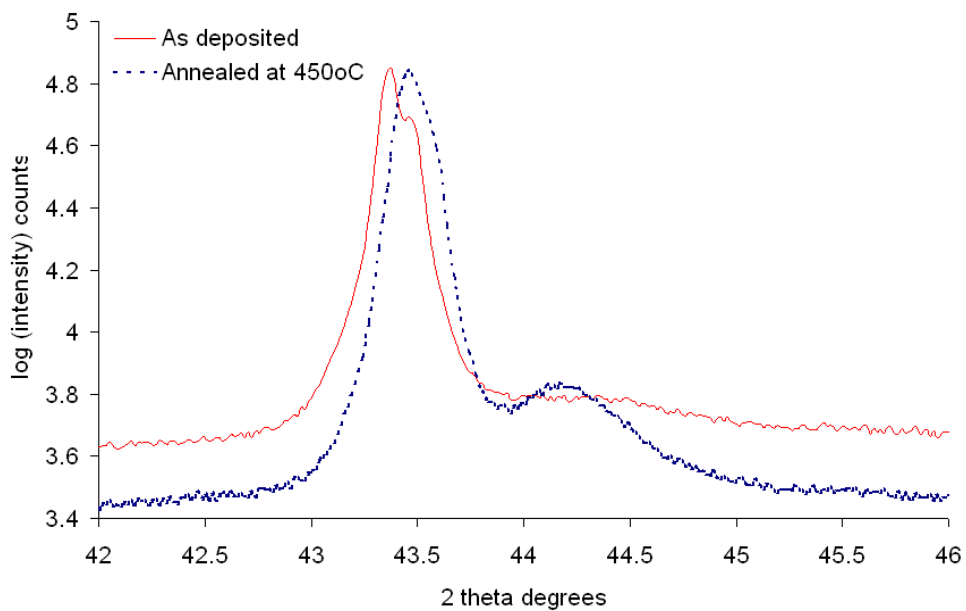


Figure 6. XRD of  $\text{Co}_{55}\text{Ni}_{20}\text{Fe}_{25}$  as deposited and following an anneal for 5 hours at  $450^\circ\text{C}$ .

## References.

1. E. J. O'Sullivan, E. I. Cooper, L. T. Romankiw, K. T. Kwietniak, P. L. Trouilloud, J. Horkans, C. V. Jahnes, I. V. Babich, S. Krongelb, S. G. Hegde, J. A. Tornello, N. C. LaBianca, J. M. Cotte, T. J. Chainer, *IBM J. Res. Dev.* 42 (1998) 681
2. C. Liu, T. Sao, G. B. Lee, J. T. S. Leu, Y. W. Yi, Y. C. Tai, C. M. Ho, *Sensors Actuat. A* 78 (1999) 190
3. W. P. Taylor, O. Brand, M. G. Allen, *J. Microelectromech.* 7 (1998) 181
4. N. Wang, T. O'Donnell, S. Roy, M. Brunet, P. McCloskey, S. C. O'Mathuna, *J. Magn. Mater.* 290–291 (2005) 1347
5. J-Y. Park, M. G. Allen, *IEEE Trans. Electron. Packag. Manuf.* 23 (2000) 48
6. M. Brunet, T. O'Donnell, L. Baud, N. Wang, J. O'Brien, P. McCloskey, S. C. O'Mathuna, *IEEE Trans. Magn.* 38 (2002) 3174
7. S. Prabhakaran, T. O'Donnell, C. R. Sullivan, M. Brunet, S. Roy, C. O'Mathuna, *J. Magn. Mater.* 290–291 (2005) 1343
8. S. Roy, A. Connell, M. Ludwig, T. O'Donnell, M. Brunet, N. Wang, P. McCloskey, C. O'Mathuna, A. Barman, R. J. Hicken; *J. Magn. Mag. Mat.* 290-291 (2005) 1524
9. T. Osaka, M. Takai, K. Hayashi, K. Ohashi, M. Saito, K. Yamada, *Nature* 392 (1998) 796
10. Y. K. Kim, H. Son, Y. S. Choi, K. S. Moon, K. H. Sunwoo, *J. Appl. Phys.* 87 (2000) 5413
11. P. E. Rasmussen, J. T. Ravnkilde, P. T. Tang, O. Hansen, S. Bouwstra, *Sensor Actuat. A* 92 (2001) 242
12. I. Tabakovic, V. Inturi, S. Riemer, *J. Electrochem. Soc.* 149 (2002) C18

13. N. Mattoso, V. Fernandes, M. Abbate, W. H. Schreiner, D. H. Mosca, *Electrochem. Solid St.* 4 (2001) C20
14. F. Lallemand, L. Ricq, P. Berçot, J. Pagetti, *Electrochim. Acta.* 47 (2002) 4149
15. R. M. Bozorth, *Ferromagnetism*, Vol. V, Van Nostrand, New York, 1951.
16. T. Osaka, *Electrochim. Acta.* 47 (2001) 23
17. D. C. Jiles, *Acta Mater.* 51 (2003) 5907
18. F. M. F. Rhen, S. Roy, *J. Appl. Phys.* 103 (2008) 103901
19. T. Homma, Y. Sezai, T. Osaka, *Electrochim. Acta* 42 (1997) 3041
20. T. Yokoshima, D. Kaneko, M. Akahori, H. S. Nam, T. Osaka, *J. Electroanal. Chem.* 491 (2000) 197
21. T. Yokoshima, S. Makamura, D. Kaneko, T. Osaka, S. Takefusa, A. Tanaka, *J. Electrochem. Soc.* 149 (2002) C375
22. T. S. N. Sankara Narayanan, S. Selvakumar, A. Stephen, *Surf. Coat. Tech.* 172 (2003) 298
23. S. K. Murthy, J. K. Vemagiri, R. A. Gunasekaran, P. Coane, K. Varahramyan. *J. Electrochem. Soc.* 151 (2004) C1
24. M. Yoshino, Y. Kikuchi, A. Sugiyama, T. Osaka, *Electrochim. Acta* 53 (2007) 285
25. L. C. Nagle, J. F. Rohan, *Electrochem. Solid St.* 8 (2005) C77
26. T. Saito, E. Sato, M. Matzuoka, C. Iwakura, *J. Appl. Electrochem.* 28 (1998) 559
27. L.C.Nagle, J.F.Rohan, *J. Electrochem. Soc.* 153 (2006) C773
28. H-S. Nam, T. Yokoshima, T. Nakanishi, T. Osaka, Y. Yamazaki, D. N. Lee, *Thin Solid Films* 384 (2001).288
29. J. F. Rohan, P. A. Murphy, J. Barrett, *J. Electrochem. Soc.* 152 (2005) C32
30. M. Saito, N. Ishiwata, K. Ohashi, *J. Electrochem. Soc.* 149 (2002) C642